Interannual Variability of the Bimodal Distribution of Summertime Rainfall Over Central America and Tropical Storm Activity in the Far-Eastern Pacific

Scott Curtis
Joint Center for Earth Systems Technology
University of Maryland, Baltimore County
Department of Geography
NASA / Goddard Space Flight Center

submitted to Climate Research

Revised March 19, 2002

Abstract

The summer climate of southern Mexico and Central America is characterized by a mid-summer drought (MSD), where rainfall is reduced by 40% in July as compared to June and September. A mid-summer reduction in the climatological number of eastern Pacific tropical cyclones has also been noted. Little is understood about the climatology and interannual variability of these minima. The present study uses a novel approach to quantify the bimodal distribution of summertime rainfall for the globe and finds that this feature of the annual cycle is most extreme over Pan America and adjacent oceans. One dominant interannual signal in this region occurs the summer before a strong winter El Niño/Southern Oscillation (ENSO). Before El Niño events the region is dry, the MSD is strong and centered over the ocean, and the mid-summer minimum in tropical cyclone frequency is most pronounced. This is significantly different from Neutral cases (non-El Niño and non-La Niña) when the MSD is weak and positioned over the land bridge. The MSD is highly variable for La Niña years, and there is not an obvious mid-summer minimum in the number of tropical cyclones.

Submitted to Climate Research
3/19/02

POPULAR SUMMARY

Interannual Variability of the Bimodal Distribution of Summertime Rainfall Over Central America and Tropical Storm Activity in the Far-Eastern Pacific

by

Scott Curtis JCET/UMBC

Most of southern Mexico and Central America's rainfall occurs in the summer months. Some of this rainfall comes from tropical storms in the eastern Pacific. Both the seasonal rainfall and number of storms have a mid-summer minimum. The reason for this minimum is not known, however one hypothesis suggests it is a response to local changes in sea surface temperature and surface winds. This study was able to objectively define the strength of the minimum. The strongest mid-summer minimum in rainfall (also known as a mid-summer drought) in the whole world occurs off the west coast of Central America.

This study also examined how the mid-summer drought in this region changed with El Niño, La Niña, and Neutral (non-El Niño and non-La Niña) summers. The biggest difference was between El Niño and Neutral cases. The mid-summer droughts tended to be weak and centered over land for Neutral summers and strong and centered over the Pacific for El Niño summers. A relationship between rainfall and tropical storm activity was shown for all cases. It appears that tropical storms contribute a lot of rain in September during El Niño and La Niña. This study suggests that El Niño brings drought to the area in the middle of summer and local effects are not as important, whereas for Neutral years the effects of clouds and precipitation on their environment produce a weak mid-summer minimum in rainfall.

1. Introduction

The climatology and interannual variability of summertime precipitation over Mexico and the Southwest U.S. (also referred to as the North American monsoon) has received increased attention in recent years (eg. Adams and Comrie 1997, Higgins et al. 1999). Applicable to this body of work, Magaña et al. (1999) described a bimodal distribution of precipitation over southern Mexico and Central America during the summer months. They showed that the mid-summer drought (MSD) is forced by the seasonal fluctuation of sea surface temperature (SST). Regional climate studies have also noted bimodal distributions of summertime precipitation, resulting from different forcing mechanisms, in the upper Midwest of the U.S. (Keables 1989) and at the Equator (Hartmann 1993). However, a globally uniform climatological analysis of intraseasonal precipitation variability has not been performed.

The typical evolution of precipitation anomalies over Mexico leading up to a mature El Niño is below normal rainfall during the monsoon season (Higgins et al. 1999), followed by above normal rainfall in autumn (Ropelewski and Halpert 1986). The 1997-1998 El Niño was a special case as the summer drought in Mexico extended into winter (Bell et al. 1999).

Magaña et al. (1999) found that the MSD appears regardless of the phase of the El Niño/Southern Osciallation (ENSO) and that there was no concurrent relationship

between the MSD and ENSO. However, summertime (June-July-August) rainfall over Mexico shows little correlation with ENSO during the same season, but a significant correlation with the following winter (December-January-February) conditions (Table 1). Thus, in this study the focus is on the relationship between the summer rainy season and the state of ENSO the following winter.

While eastern Pacific tropical storms play an important role in the North American monsoon system (eg. Higgins and Shi 2001), extreme events can be very costly to the people of Mexico's west coast. The ratio of tropical storm rainfall to total rainfall in southwestern Mexico ranges from 10 to 40% (Englehart and Douglas 2001). These values exceed 50% in the vicinity of the Baja peninsula (Rodgers et al. 2000, Englehart and Douglas 2001).

Attempts have been made to relate the seasonal statistics of eastern Pacific tropical cyclones to ENSO. Whitney and Hobgood (1997) found no ENSO related impact on the number, intensity, or track length of tropical storms. Irwin and Davis (1999) showed that storms originated about 6° longitude to the west of normal during strong El Niño events. This is consistent with Englehart and Douglas (2001) who found that tropical storm related rainfall at stations on Mexico's southwest coast decreased during El Niño events. However, Rodgers et al. (2000), using satellite data, showed that tropical cyclone rainfall was enhanced over the far-eastern Pacific for El Niño versus La Niña summers.

Most intraseasonal diagnostics of tropical cyclone activity have focused on the Madden Julian Oscillation (MJO) which has a 30-60 day periodicity (eg. Maloney and Hartmann 2000). Magaña et al. (1999) described a mid-summer minimum in the frequency of storms over the eastern Pacific warm pool as a signature of the MSD. However, questions remain as to the relationship of the bimodal nature of tropical cyclone activity to the intraseasonal rainfall variability. Also, no studies (to my knowledge) have examined the interannual variability of the bimodal distribution of eastern Pacific tropical storms.

A state-of-the-art precipitation data set will be introduced and a method will be described to quantify the bimodal nature of precipitation and number of named storms in section 2. The intraseasonal variability of precipitation over Mexico and Central America and number of tropical storms in the far-eastern Pacific will be analyzed in terms of ENSO in sections 3 and 4. The sea surface temperature (SST) forcing mechanism will be examined in section 5. Finally, a summary of the results and a discussion of other factors that may contribute to the different intraseasonal variations during El Niño, La Niña, and Neutral summers will be presented in section 6.

2. Data and Methods

Intraseasonal precipitation information is obtained from the Global Precipitation Climatology Project (GPCP) pentad (5-day) 2.5° latitude by 2.5° longitude data (Xie et

al. 2002). This data set, spanning the period 1979 to present, is similar to the Climate Prediction Center's Merged Analysis of Precipitation (CMAP; Xie and Arkin 1997) except the pentad precipitation estimates are adjusted to sum to the GPCP Version 2 monthly product (Adler et al., 2002). The GPCP pentad product is a merger of various satellite estimates and gauge information and is of higher quality compared to individual data sources.

Weekly National Center for Environmental Prediction (NCEP) sea surface temperature anomalies (Reynolds and Smith 1994) at 1 degree latitude by 1 degree longitude resolution were averaged into an east Pacific warm pool index (105°W - 95°W, 10°N - 15°N).

Tropical storm and hurricane track information was downloaded from the National Hurricane Center web site (http://www.nhc.noaa.gov). Storms located in the Pacific Ocean east of 110° W were counted once on the day they originated, and the counts were summed over 10-day (2 pentad) intervals from May 1-10 to October 28 - November 6. This was done to ensure consistency with the GPCP data.

The ENSO Precipitation Index (ESPI; Curtis and Adler 2000), a monthly measure of the zonal gradient of precipitation anomalies between the central equatorial Pacific (10°S - 10°N; 160°E - 100°W) and the Maritime Continent (10°S - 10°N; 90°E - 150°E), was used to define ENSO events. ESPI is highly correlated to traditional measures of

ENSO such as the Nino 3.4, however ESPI is more closely connected to the large-scale circulation as forced by warm and cold SST events.

A simple objective method was devised for quantifying the bimodal nature of May to October precipitation and number of tropical cyclones. The first order harmonic (FOH) from the normalized variance spectrum of a time series yields a sinusoidal wave with one peak and one trough. For the case of the precipitation data, if the peak (trough) is near the center of the time range, then the FOH represents a rainy season (dry season) (Fig. 1). The second order harmonic (SOH) yields a sinusoidal wave with two peaks and two troughs. Only in the special case where one of the troughs is very close to the beginning (early May) or end (late October) of the record, does the SOH represent the mid-summer minimum condition (Fig. 1). The time series of precipitation and number of tropical cyclones are actually composed of the FOH, SOH, and other higher frequency oscillations. This paper is only concerned with the relative strengths of the SOH.

3. The Mid-Summer Drought

A 21-year climatology (1979 to 1999) of pentad precipitation was constructed for May 1-5 to October 28-November 1. The normalized variance spectrum was computed for each grid block and the variance explained by the SOH was plotted (Fig. 2). Areas such as coastal China and southern Japan show some power in this mode. However, the SOH is strongest in the Pan American region, where the MSD has been historically

observed, suggesting that the SOH is a good statistical model for this phenomenon of the annual cycle. The SOH explains over 30% of the variance of summertime precipitation over much of southern Mexico, Central America, and surrounding oceans, and explains over 50% of the variance over Guatemala and El Salvador (Figs. 2, 3a).

Next the summers from 1979 to 1999 were categorized by the ESPI value of the following Decemeber-January-February (DJF). El Niño summers were defined as 1982, 86, 89, 91, 92, 94, and 97 (average ESPI value: 0.97), La Niña summers as 1983, 84, 85, 88, 95, 98, and 99 (average ESPI value: -0.98), and Neutral summers as 1979, 80, 81, 87, 90, 93, and 96 (average ESPI value: -0.32). The same spectral analysis was performed on the three composites of precipitation. The SOH is equally strong for El Niño years (Fig. 3b) as compared to climatology (Fig. 3a), but the bulk of the values have shifted westward over the ocean. For the La Niña (Fig. 3c) and Neutral (Fig. 3d) composites the power of the SOH is reduced substantially. Also, in the Neutral case, values in excess of 20% are centered over land (Fig. 3d).

To test whether the differences between the El Niño composite and non-El Niño composites are significant the power of the SOH for precipitation values averaged over the core of the MSD region (Fig. 3) was computed for each year. The time series of the variance explained by the SOH is given in Fig. 4. The La Niña years have a mean value equivalent to the climatological mean (0.20) and a large standard deviation. In fact, the year with the lowest power (1985) and the year with the highest power (1999) are La

Niña years. Five out of the seven El Niño years have power above the mean and six out of the seven Neutral years have power below the mean. A two-tailed t-test shows that the El Niño years and Neutral years are significantly different at the 95% confidence level ($t = 2.4$ and $p = 0.033$).

4. The Mid-Summer Minimum in Tropical Cyclones

In this section the number of named tropical cyclones originating to the east of 110° W (dashed line in Fig. 3) is examined from May to October. Fig. 5a shows a bimodal distribution, consistent with Magaña et al. (1999)'s results. From 1979 to 1999 a relative minimum in named storms occurred in the middle of August. However, the SOH of the time series explains less of the variance (23.5%) than the FOH (67.6%) suggesting that the time series of tropical cyclone frequency has one rather than two distinct peaks in the distribution. For comparison, the climatological precipitation for the core of the MSD region (Fig. 3) is presented. Rainfall shows a pronounced bimodal distribution, reduced by roughly 40% in late July as compared to June and September. Also, the power of the SOH is twice as large as the power of the FOH (62.6% versus 31.3% of the variance). The MSD leads the August minimum in tropical cyclones.

As in section 3, the number of tropical cyclones was divided into El Niño, La Niña, and Neutral composites. For the El Niño composite (Fig. 5b) the variance explained by SOH increased to 30.1%, approaching the variance explained by the FOH

(49.1%). Besides the local maximum in early August, the two peaks in the distribution occur in early July and late September. The second and larger peak is at the same time as the heaviest rainfall during an average El Niño summer. The summertime frequency of named storms during La Niña events (Fig. 5c) is not bimodal. Peaks in early July, late July, early August, and early September dominate the distribution. The MSD is also weak, as the early season precipitation maximum is not well defined. The first and second harmonics explain about equal amounts of the variance (40.5% versus 38.1%) for the precipitation time series. For Neutral years (Fig. 5d) there is a weak bimodal signal in storm frequency and rainfall. The late season peaks are damped as compared to the ENSO composites. The total number of tropical cyclones for the El Niño, La Niña and Neutral years are 82, 80, and 75 respectively. These numbers are not significantly different, supporting the results of Whitney and Hobgood (1997).

5. Sea Surface Temperatures

Magaña et al. (1999) show that sea surface temperatures decrease over the eastern Pacific warm pool in July or August in response to increases in convective activity and changes in wind patterns. Here the same data (see section 2) is examined, but separated into extreme wintertime ENSO events.

In the El Niño summer the waters are anomalously warm until late September when there is a sudden return to normal conditions (Fig. 6a). The La Niña summer shows

a slow decline in SST from June to October (Fig. 6b). Finally, observations during Neutral summers show the greatest resemblance to Magaña et al. (1999)'s 1982-93 climatology. SSTs are high in June, briefly decline in July-August, and increase into September-October (Fig. 6c).

6. Discussion and Summary

While wintertime ENSO is highly correlated with the previous June-July-August precipitation in the Mexican monsoon region (Table 1), there is no correlation at the beginning (May) and end (September) of the monsoon (0.05 and -0.01 respectively). Thus, early during El Niño summers the waters warm and precipitation increases simultaneously, as described by Magaña et al. (1999). However, the mid-summer drought (MSD) and mid-summer minimum in tropical cyclone development appear despite continued high temperatures. These minima are likely responding to changes in the large-scale circulation. The El Niño induced drought in the region is strongest in the middle of the summer season (Table 1) when the convection associated with the ITCZ is weakest and furthest south (Curtis et al. 1999). In September the storms return along with enhanced rainfall, blocking incoming solar radiation and reducing the SST. The net effect is the strongest MSD, in terms of percent decrease of mid-summer rainfall, as compared to Neutral or La Niña years.

The beginning of a typical La Niña summer behaves the same way as an El Niño summer, but instead of southward, the ITCZ shifts north leading to a slow decline in SST and a small decrease in precipitation. Neither the rainfall nor number of named storms shows an obvious mid-summer minimum. Irwin and Davis (1999) found that more tropical cyclones originate and remain near the Mexican coast during La Niña. The end of the summer is also similar between El Niño and La Niña events. In September rainfall increases substantially, possibly tied to enhanced tropical cyclone activity. Sixteen named storms from August 29 to September 17 were identified during the seven La Niña years studied (Fig 5c). Again, the increase in clouds and rainfall diminishes the incoming solar radiation and cools the underlying waters.

Finally, observations during Neutral summers show the greatest resemblance to Magaña et al. (1999)'s proposed chain of causality for the MSD. Increasing precipitation during June leads to a drop in SST; consequently inhibiting rainfall in July-August and allowing increased solar radiation to warm the waters, which is followed by the return of precipitation in September. Magaña et al. (1999)'s dynamical explanation also involves changes to the surface convergence, not examined here.

In summary, the spectral peak in the second order harmonic of boreal summer precipitation is uniquely strong over Pan America as compared to the rest of the world. An index of precipitation over Central America confirms that the second order harmonic describes the MSD phenomenon for this region. The number of tropical storms

originating east of 110° W also decreases in the middle of summer, but the second order harmonic does not explain as much of the intraseasonal power as the first order harmonic. Magaña et al. (1999) proposed local air-sea interactions in establishing the MSD. The findings presented here are consistent with this hypothesis for Neutral (non-El Niño and non-La Niña) summers. However, during El Niño and La Niña large-scale changes in circulation, namely the preferred location of the eastern Pacific ITCZ, are just as, if not more, important than local air-sea mechanisms.

Table 1. Correlations between Mexican monsoonal rainfall (95°W-110°W; 7.5°N-27.5°N) and ENSO Precipitation Index for the prior winter December-January-February (DJF(-)), concurrent summer June-July-August (JJA(0)), and following winter DJF(0).

RAIN	ENSO Precipitation Index: DJF(-)	ENSO Precipitation Index: JJA(0)	ENSO Precipitation Index: DJF(0)
June-July-August	0.26	-0.02	-0.81**
June	-0.13	-0.48	-0.45
July	0.50	-0.09	-0.34
August	0.11	-0.61*	-0.82**

*Significance at the 5% level; **Significance at the 1% level

Figure Captions

Figure 1. Examples of harmonic models to precipitation data. Thin solid and dashed lines represent wet and dry seasons respectively, as modeled by the first order harmonic. Heavy solid line represents a bimodal distribution of precipitation (with a minimum centered in the middle of the season), as modeled by the second order harmonic.

Figure 2. Variance explained by the second order harmonic for climatological (1979-1999) May to October global precipitation. Shading increases with the contour levels: 0.2, 0.3, 0.4, and 0.5.

Figure 3. Same as Figure 2, except restricted to the Pan American region. A) 1979-1999 climatology, B) El Niño (1982, 1986, 1989, 1991, 1992, 1994, and 1997), C) La Niña (1983, 1984, 1985, 1988, 1995, 1998, and 1999), and D) Neutral (1979, 1980, 1981, 1987, 1990, 1993, and 1996). Boxes indicate area over which mean precipitation time series were computed for Figures 4 and 5. Dashed line marks the western boundary of the Pacific tropical cyclone search area.

Figure 4. Variance explained by the second order harmonic for May to October precipitation averaged over the box in Figure 3. Closed circles represent El Niño years, open circles La Niña years, and 'X's Neutral years. The average variance explained for each category is given in the legend box.

Figure 5. Solid line denotes the May to October time series of precipitation (mm/day) averaged over the box in Figure 3. Open bars indicate number of named storms observed in the North Pacific east of 110° W. A) 1979-1999 climatology, B) El Niño (1982, 1986, 1989, 1991, 1992, 1994, and 1997), C) La Niña (1983, 1984, 1985, 1988, 1995, 1998, and 1999), and D) Neutral (1979, 1980, 1981, 1987, 1990, 1993, and 1996). The variance explained (in hundredths) by the second order harmonic for the rainfall (RAIN) and tropical storm (TS) time series are given in the upper left-hand corners.

Figure 6. The weekly SST anomaly averaged over the eastern Pacific warm pool (10°-15°N; 105°-95°W) for May to October. A) Solid lines denote 1982, dotted lines 1991, and dashed lines 1997, B) Solid lines denote 1983, dotted lines 1995, and dashed lines 1999, C) solid lines denote 1987, and dotted lines 1990.

References

Adams, D. K., and A. C. Comrie, 1997: The North American monsoon. *Bull. Amer. Meteor. Soc.*, 78, 2197-2213.

Adler, R. F., G. J. Huffman, A. Chang, R. Ferraro, P. Xie, J. Janowiak, B. Rudolf, U. Schneider, S. Curtis, D. Bolvin, A. Gruber, J. Susskind, and P. Arkin, 2002: The version 2 Global Precipitation Climatology Project (GPCP) monthly precipitation analysis (1979-present). *J. Hydrometeor.*, submitted.

Bell, G. D., M. S. Halpert, C. F. Ropelewski, V. E. Kousky, A. V. Douglas, R. C. Schnell, and M. E. Gelman, 1999. Climate assessment for 1998. *Bull. Amer. Meteor. Soc.*, 80, S1-S48.

Curtis, S., and R. Adler, 2000: ENSO indices based on patterns of satellite derived precipitation. *J. Climate*, 13, 2786-2793.

Curtis, S., R. Adler, G. Huffman, D. Bolvin, and E. Nelkin, 1999: Global precipitation patterns associated with ENSO and tropical circulations: ENSO and the summer monsoons over southern Asia and Mexico. *Proceedings of the Twenty fourth Climate Diagnostics and Prediction Workshop*, 142-144.

Englehart, P. J., and A. V. Douglas, 2001: The role of eastern North Pacific tropical storms in the rainfall climatology of western Mexico. *Int. J. Climatol.*, 21, 1357-1370.

Higgins, R. W., Y. Chen, and A. V. Douglas, 1999: Interannual variability of the North American warm season precipitation regime. *J. Climate*, 12, 653-680.

Higgins, R. W., and W. Shi, 2001: Intercomparison of the principal modes of interannual variability of the North American Monsoon System. *J. Climate*, 14, 403-417.

Hartmann, D., 1993: *Global Physical Climatology*. Academic Press, 411 pp.

Irwin, R. P., and R. E. Davis, 1999: The relationship between the Southern Oscillation Index and tropical cyclone tracks in the eastern North Pacific. *Geophys. Res. Letters*, 26, 2251-2254.

Keables, M., 1989: A synoptic climatology of the bimodal precipitation distribution in

the upper Midwest. *J. Climate*, 2, 1289-1294.

Magaña, V., J. A. Amador, and S. Medina, 1999: The midsummer drought over Mexico and Central America. *J. Climate*, 12, 1577-1588.

Maloney, E. D., and D. L. Hartmann, 2000: Modulation of eastern North Pacific Hurricanes by the Madden-Julian Oscillation. *J. Climate*, 13, 1451-1460.

Reynolds, R., and T. Smith, 1994: Improved global sea surface temperature analyses using optimum interpolation. *J. Climate*, 7, 929-948.

Rodgers, E. B., R. F. Adler, and H. F. Pierce, 2000: Contribution of tropical cyclones to the North Pacific climatological rainfall as observed from satellites. *J. Appl. Meteor.*, 39, 1658-1678.

Ropelewski, C. F., and M. S. Halpert, 1986: North American precipitation and temperature patterns associated with the El Niño/ Southern Osciallation (ENSO). *Mon. Wea. Rev.*, 114, 2352-2362.

Whitney, L. D., and J. S. Hobgood, 1997: The relationship between sea surface temperatures and maximum intensities of tropical cyclones in the eastern North Pacific Ocean. *J. Climate*, 10, 2921-2930.

Xie, P., and P. A. Arkin, 1997: Global precipitation: A 17-year monthly global analysis based on gauge observations, satellite estimates, and numerical model outputs. *Bull. Amer. Meteor. Soc.*, 78, 2539-2558.

Xie, P., J. E. Janowiak, P. A. Arkin, R. F. Adler, A. Gruber, R. Ferraro, G. J. Huffman, and S. Curtis, 2002: GPCP pentad precipitation analyses: An experimental data set based on gauge observations and satellite estimates. *J. Hydrometeor.*, submitted.

FIG 1

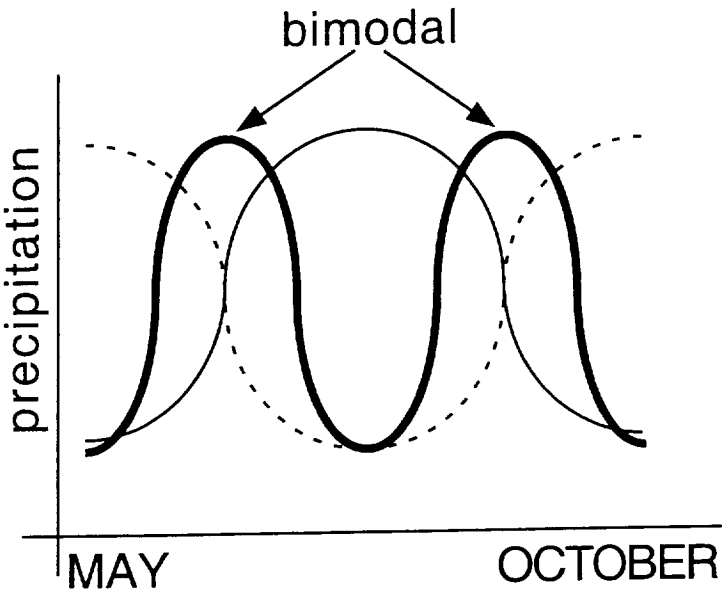

FIG 2

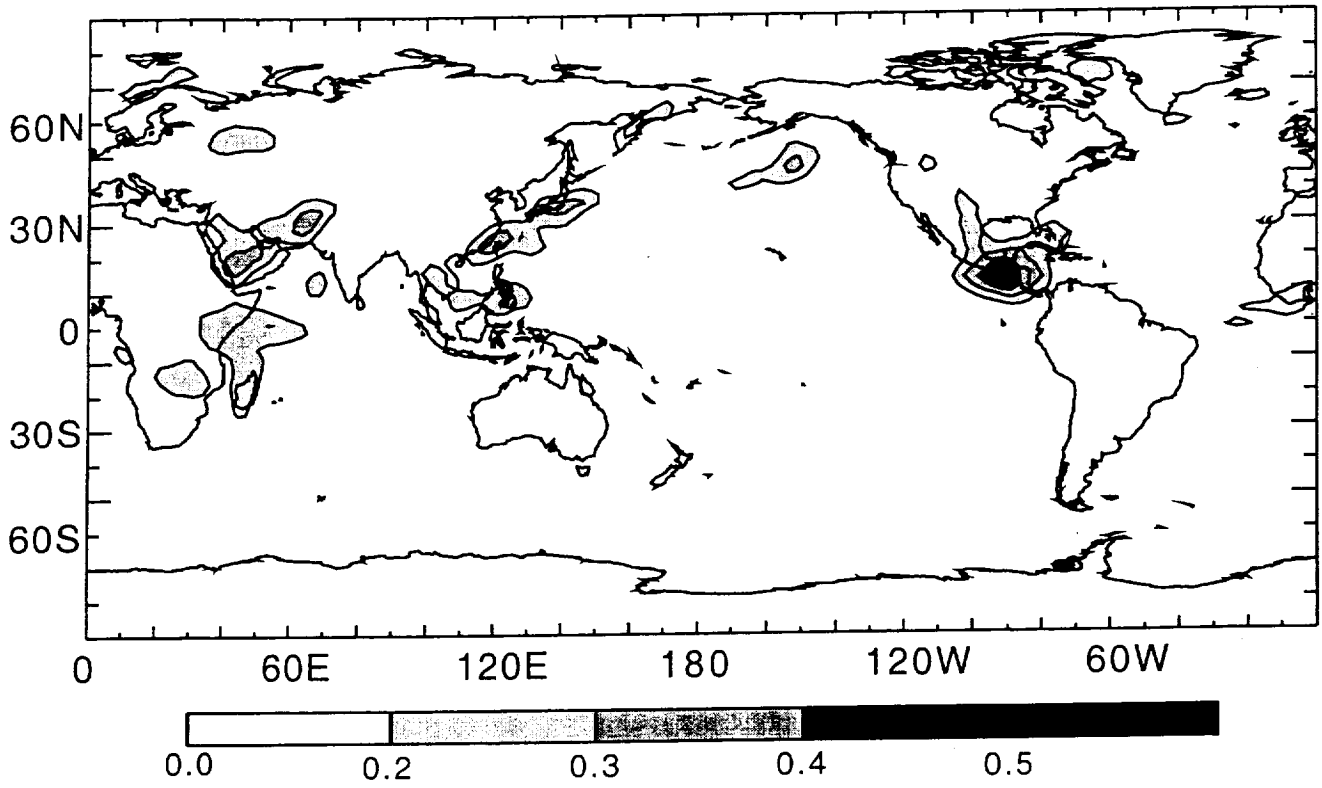

FIG 3.

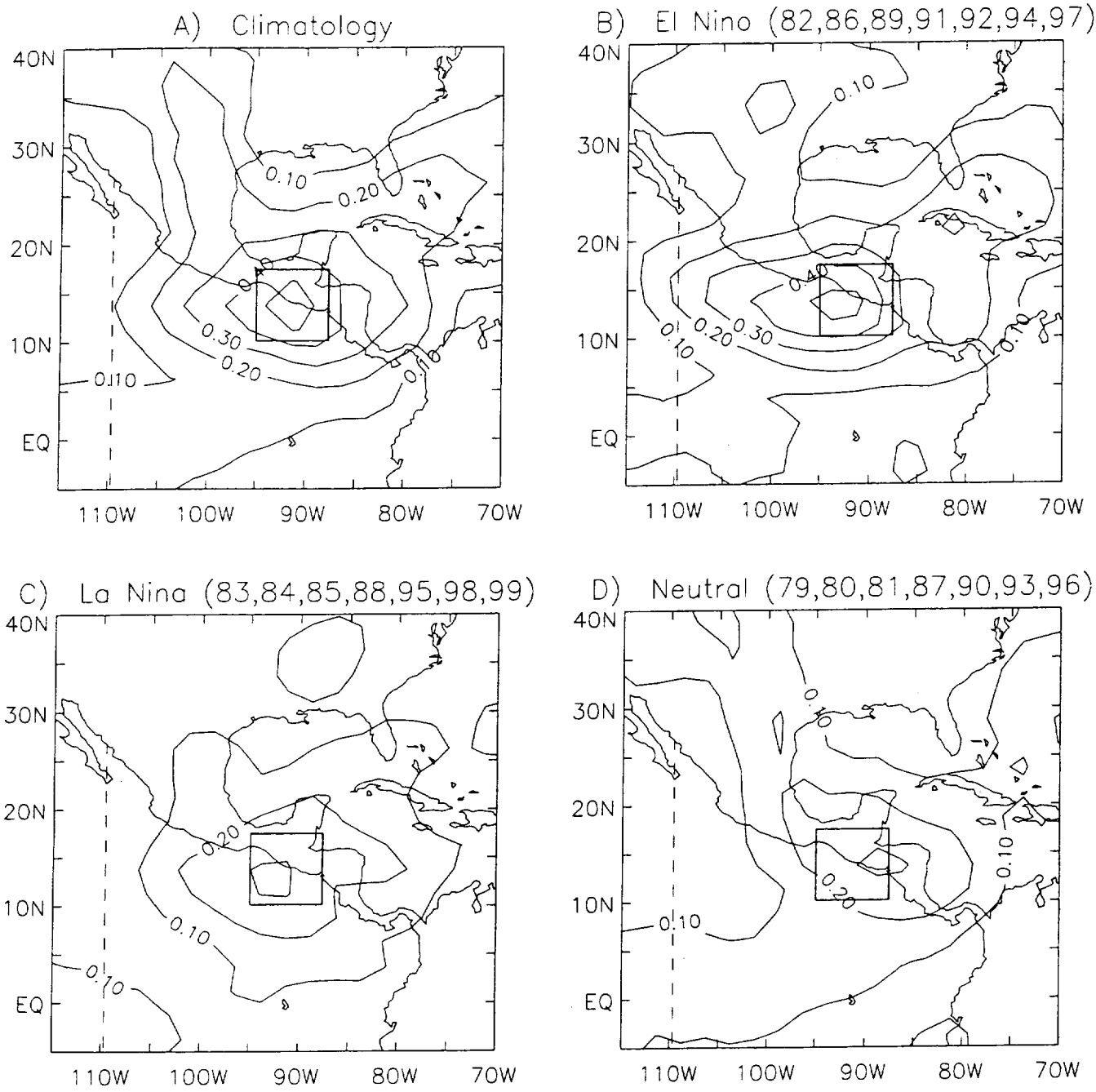
A) Climatology
40N
30N
20N
10N
EQ
110W
100W
90W
80W
70W
0.10
0.20
0.30
0.20
0.10
B) El Nino (82,86,89,91,92,94,97)
0.10
0.10
0.20
0.30
0.10
C) La Nina (83,84,85,88,95,98,99)
0.20
0.10
0.10
D) Neutral (79,80,81,87,90,93,96)
0.10
0.10
0.10

FIG 4

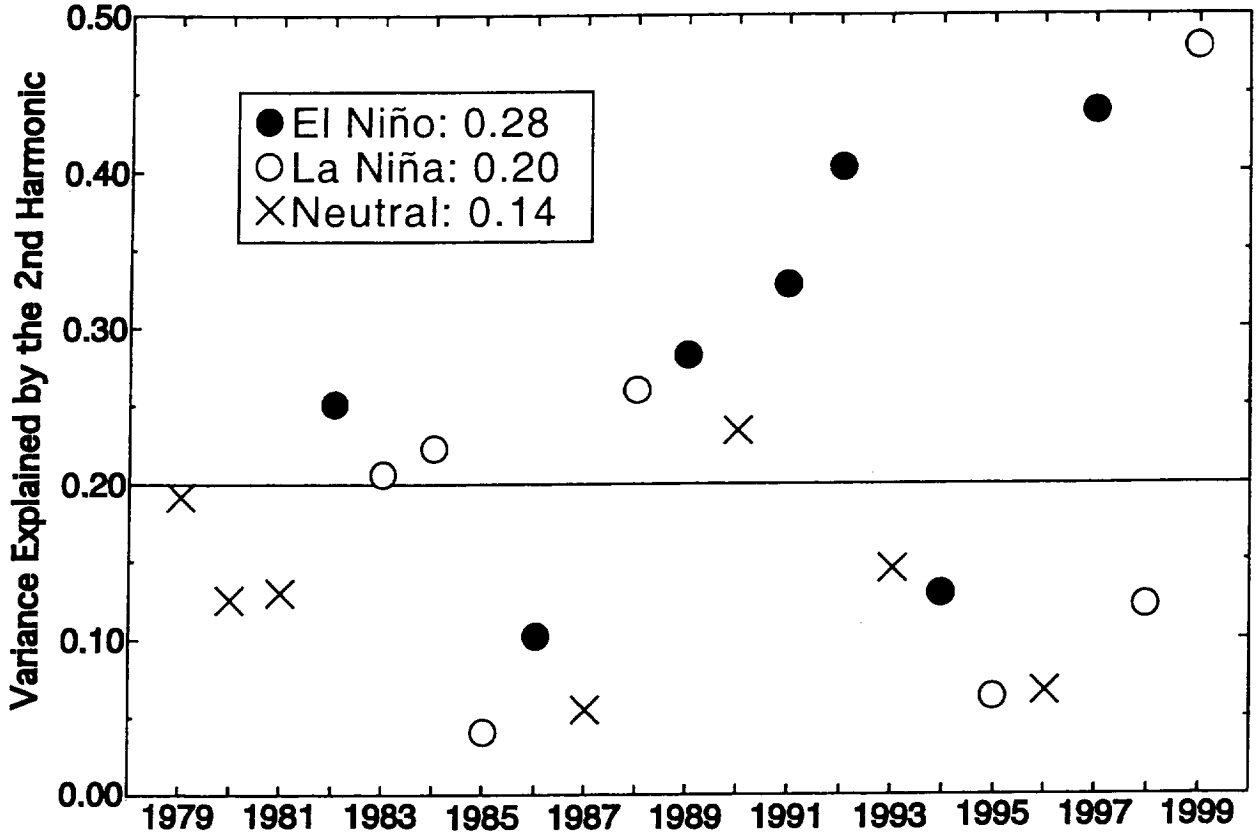
Variance Explained by the 2nd Harmonic
0.50
0.40
0.30
0.20
0.10
0.00
El Niño: 0.28
La Niña: 0.20
Neutral: 0.14
1979
1981
1983
1985
1987
1989
1991
1993
1995
1997
1999

FIG 5

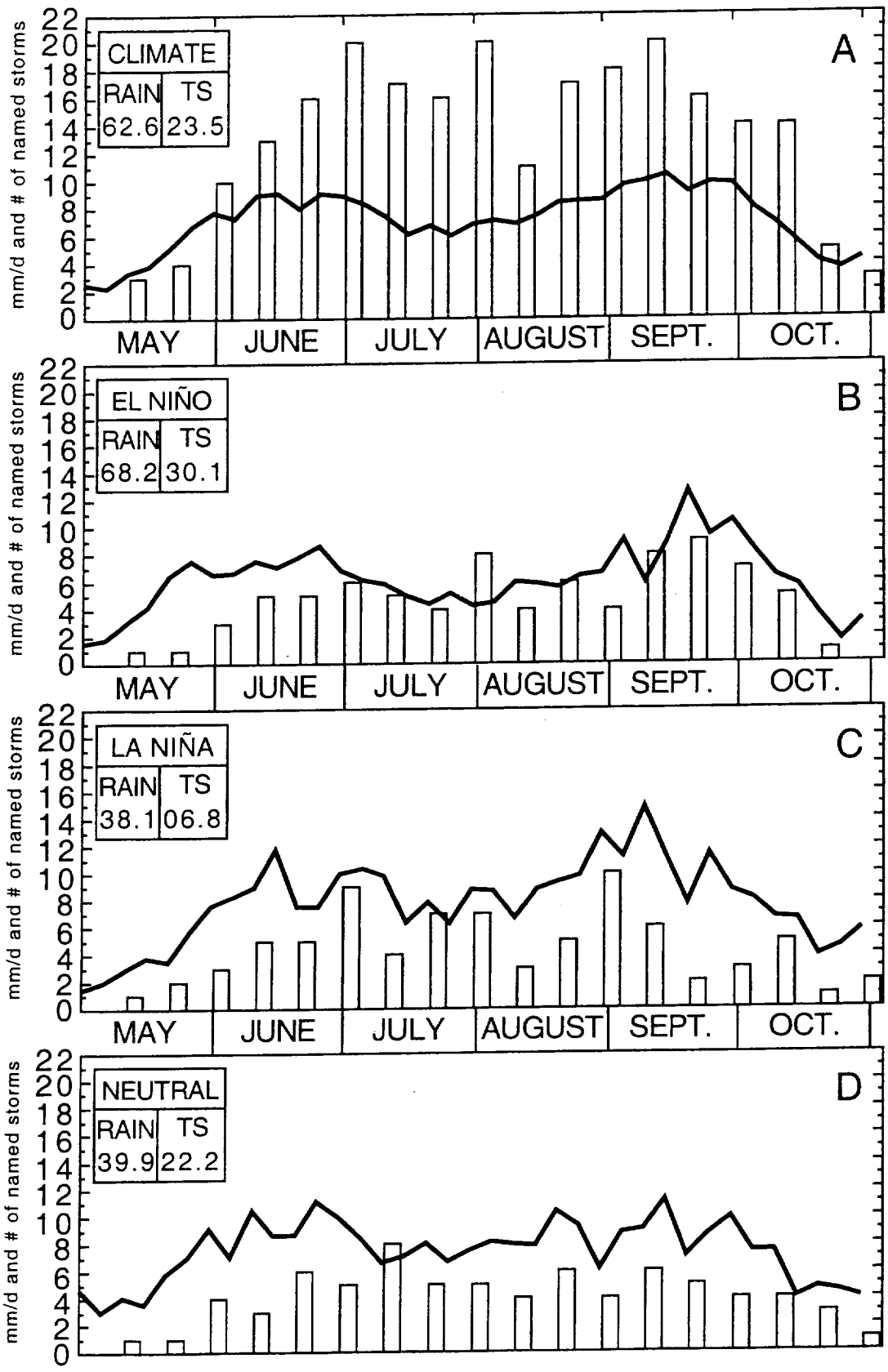
mm/d and # of named storms
22
20
18
16
14
12
10
8
6
4
2
0
CLIMATE
RAIN 62.6
TS 23.5
A
MAY
JUNE
JULY
AUGUST
SEPT.
OCT.
EL NIÑO
RAIN 68.2
TS 30.1
B
LA NIÑA
RAIN 38.1
TS 06.8
C
NEUTRAL
RAIN 39.9
TS 22.2
D

FIG 6

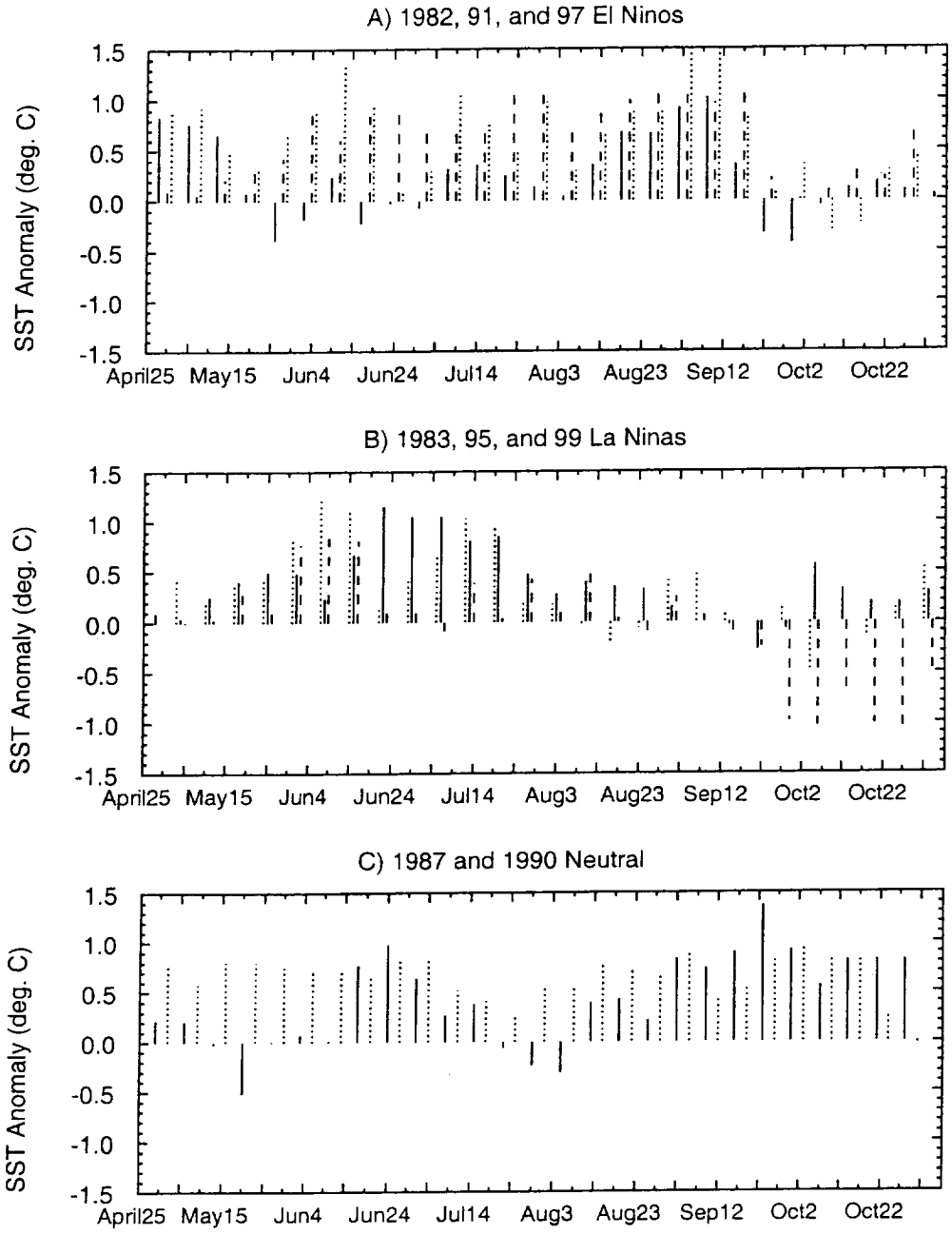
A) 1982, 91, and 97 El Ninos
SST Anomaly (deg. C)
1.5
1.0
0.5
0.0
-0.5
-1.0
-1.5
April25
May15
Jun4
Jun24
Jul14
Aug3
Aug23
Sep12
Oct2
Oct22
B) 1983, 95, and 99 La Ninas
SST Anomaly (deg. C)
1.5
1.0
0.5
0.0
-0.5
-1.0
-1.5
April25
May15
Jun4
Jun24
Jul14
Aug3
Aug23
Sep12
Oct2
Oct22
C) 1987 and 1990 Neutral
SST Anomaly (deg. C)
1.5
1.0
0.5
0.0
-0.5
-1.0
-1.5
April25
May15
Jun4
Jun24
Jul14
Aug3
Aug23
Sep12
Oct2
Oct22